

## A Facile Strategy to Prepare Cu<sub>2</sub>O/Cu Electrode as a Sensitive Enzyme-free Glucose Sensor

Li Wang<sup>1,2</sup>, Jinying Fu<sup>2</sup>, Haoqing Hou<sup>2</sup> and Yonghai Song<sup>1,2,\*</sup>

<sup>1</sup> Key Laboratory of Functional Small organic molecule, Ministry of Education, Jiangxi Normal University, Nanchang 330022, People's Republic of China

<sup>2</sup> College of Chemistry and Chemical Engineering, Jiangxi Normal University, Nanchang 330022, People's Republic of China

\*E-mail: [lwanggroup@yahoo.com.cn](mailto:lwanggroup@yahoo.com.cn)

Received: 20 October 2012 / Accepted: 5 November 2012 / Published: 1 December 2012

---

A Cu<sub>2</sub>O/Cu electrode was fabricated by applying an anodic voltage to the Cu electrode in a mixed alcohol–water solution containing 1,3,5–benzentricarboxylic acid and NaClO<sub>4</sub>. The Cu<sub>2</sub>O/Cu electrode was characterized by scanning electron microscopy, X–ray powder diffraction and electrochemical technique. The results showed that ultrafine Cu<sub>2</sub>O microcrystal was densely assembled on the Cu electrode and as-prepared Cu<sub>2</sub>O/Cu electrode exhibits large surface area. The resulted sensor showed high catalytic activity towards the oxidation of glucose with a wide linear range of 0.05–6.75 mM and detection limit of 37 μM. The good catalytic activity, high sensitivity and good stability made such Cu<sub>2</sub>O/Cu electrode to be a promising candidate for constructing novel enzyme-free sensor.

---

**Keywords:** Cu<sub>2</sub>O/Cu electrode; electrocatalytic oxidation; glucose; enzyme-free sensor

### 1. INTRODUCTION

Glucose, as an essential physiological component, distributes extensively in blood of living beings, foods and pharmaceuticals [1]. It is often used as a marker of diabetes which has become one of the major health afflictions worldwide [2]. Therefore, the quantitative determination of glucose level not only in blood but also in other sources such as foods and pharmaceuticals is very important in biological and clinical analysis [3–9].

To date, the electrochemical technique for glucose determination has attracted extensive attention owing to its high sensitivity, low cost, rapid response and compatibility for miniaturization [9–11]. Generally, the glucose determination is by monitoring the current that glucose oxidase (GOD) catalyzes the oxidation of glucose [12–14]. Despite the low detection limit and high selectivity, the use

of the GOD obviously deteriorates transducer properties due to its poor direct electrochemistry. Furthermore, enzyme-based sensor involves complicated, multi-step immobilization procedures [15]. Under critical operating conditions, the measurements suffers from poor reproducibility, thermal and chemical instability and high cost [10,16]. Environmental conditions such as temperature, pH, and humidity and the presence of ionic detergents and enzyme-poisoning molecules in the sample can easily interrupt the performance of sensors.

Mediating metal or metal oxide materials on an electrode as a catalyst, which can also determine the amount of trace glucose, is a hot topic owing to their large specific surface areas, excellent conductivities and catalytic activities. Many materials, including CuO [17-19], Cu nanoparticles (NPs) [20], CuO nanocubes [21], MnO<sub>2</sub> NPs [22], NiO nanofibers [23], ZnO nanorods [24], etc., have been widely used to construct electrochemical glucose sensors. Among these sensors, the sensor based on Cu materials exhibits an extremely fast amperometric response, low detection limit and wide linear range owing to their greater ability to promote electron-transfer reactions. A large number of studies showed that the sensor's catalytic properties depended strongly on the size, distribution and shape of Cu materials. To obtain good catalytic activity, various Cu materials have been fabricated to develop nonenzymatic glucose sensor, such as a large-scale epitaxial array of single-crystalline CuO nanowires on the surface of a Cu nanostructure [25], Cu/Cu<sub>2</sub>O hollow microspheres [26], CuO nanobelt arrays [27], Cu micropuzzles [28], CuO nanowalls on Cu substrate [29], CuS nanotubes [30,31], CuO nanowires [32], CuO NPs [15,33,34], Cu nanowires [1], electrospun Pt-doped CuO nanofibers [18], CuO/TiO<sub>2</sub> nanotube [35], electrodepositing Cu NPs on graphene sheet modified electrode [20], CuO nanocubes-graphene nanocomposite [21], CuO/Cu oxalate [19], nanospindle-like Cu<sub>2</sub>O/straight multi-walled carbon nanotubes (MWCNTs) hybrid nanostructures [36], Cu<sub>2</sub>O/polyvinyl pyrrolidone-graphene nanocomposites [37], etc. However, the synthesis of Cu materials is tedious and often involves surface immobilization. As a result, there is an unmet need for a simple, reliable, and sensitive sensor for direct nonenzymatic measurement of glucose in blood and other samples.

In this work, a facile strategy to prepare Cu<sub>2</sub>O/Cu electrode as a sensitive nonenzymatic glucose sensor was developed by applying an anodic voltage to the Cu electrode in a mixed alcohol-water (1:1) solution containing 1,3,5-benzentricarboxylic acid and NaClO<sub>4</sub>. The resulted Cu<sub>2</sub>O/Cu electrode showed good electrocatalytic ability to oxidation of glucose. The experimental conditions related to the preparation of the Cu<sub>2</sub>O/Cu electrode and the performances of the resulted sensor were investigated in detail.

## 2. EXPERIMENTAL SECTION

### 2.1 Chemicals and reagents

d(+)-Glucose, uric acid (UA), L-ascorbic acid (AA) was purchased from Aladdin. 1,3,5-benzentricarboxylic acid (BTC) were obtained from Sigma-Aldrich (Milwaukee Wisconsin). Other reagents were purchased from Beijing Chemical Reagent Factory (Beijing, China). All reagents were

of analytical grade and used without further purification. All solutions were prepared with ultra-pure water, purified by a Millipore-Q system (18.2 M $\Omega$  cm).

### 2.2 Preparation of the Cu<sub>2</sub>O/Cu electrode

The Cu<sub>2</sub>O/Cu electrode was prepared by electrochemical method [38]. The Cu electrode was polished carefully on different specifications of abrasive papers until the surface of Cu electrode was as smooth as mirror then cleaned by brief ultrasonic. A voltage was applied to the two Cu electrodes in a mixed alcohol-water (1:1) solution containing 0.01 M BTC and 0.1 M NaClO<sub>4</sub> for different times. Then Cu<sub>2</sub>O microcrystal were produced and densely compacted on cathodic Cu electrode.

### 2.3 Apparatus

The scanning electron microscopy (SEM) analysis was taken using a XL30 ESEM-FEG SEM at an accelerating voltage of 20 kV equipped with a Phoenix energy dispersive x-ray analyzer (EDXA). X-ray powder diffraction (XRD) data were collected on a D/Max 2500 V/PC X-ray powder diffractometer using Cu K $\alpha$  radiation ( $\lambda=0.154056$  nm, 40 kV, 200 mA). The preparation of electrodes was carried out with a DELIXI WYJ-30V5A DC stabilized power supply.

All electrochemical measurements were performed on a CHI 660C electrochemical workstation (Shanghai, China) at ambient temperature. A conventional three-electrode system was employed including a bare or modified Cu electrode as working electrode, a platinum wire as auxiliary electrode and a Ag/AgCl electrode (saturated KCl) as reference electrode. The cyclic voltammetric experiments were performed in a quiescent solution. The amperometric experiments were carried out under a continuous stirring. 0.1 M NaOH as the supporting electrolyte solution was purged with high purity nitrogen for 15 min prior to each measurement then a nitrogen atmosphere was kept over the solution during measurements.

## 3. RESULTS AND DISCUSSION

### 3.1 Characteristics of the Cu<sub>2</sub>O/Cu electrode

The morphology of Cu<sub>2</sub>O/Cu electrode was examined by SEM. The electrochemical formation of coatings on the surface of cathodic copper sheet was shown in Fig. 1A. It was observed that some crystals with similar octahedron shape were uniformly dispersed on the surface of the copper sheet. They were in varied sizes with different generation time. Fig. 1B and Fig. 1C show high magnification of Cu<sub>2</sub>O of different domain, respectively. Fig. 1B indicated clearly that the crystal shape was octahedron. Fig. 1C showed that the materials which have not grown into big crystal yet but already reached the shape of octahedron.

The crystal structure and the phase purity of the as-prepared Cu<sub>2</sub>O materials were further characterized by XRD and the results were shown in Fig.1D. As can be seen in the pattern, there were

a series of characteristic diffraction peaks at  $29.34^\circ$ ,  $36.51^\circ$ ,  $42.40^\circ$ ,  $61.48^\circ$  and  $73.07^\circ$ , which were indexed as the diffractions of the (110), (111), (200), (220) and (311) crystalline planes of cubic  $\text{Cu}_2\text{O}$  (JCPDS card No. 05-0667) [26,38]. And the characteristic diffraction peak at  $50.45^\circ$  was indexed as the diffraction of the (200) of Cu substrate according to the standard spectrum of Cu (JCPDS card No. 040836). No other impurities could be detected in the XRD pattern of  $\text{Cu}_2\text{O}$  materials. The results confirmed that pure  $\text{Cu}_2\text{O}$  were formed.

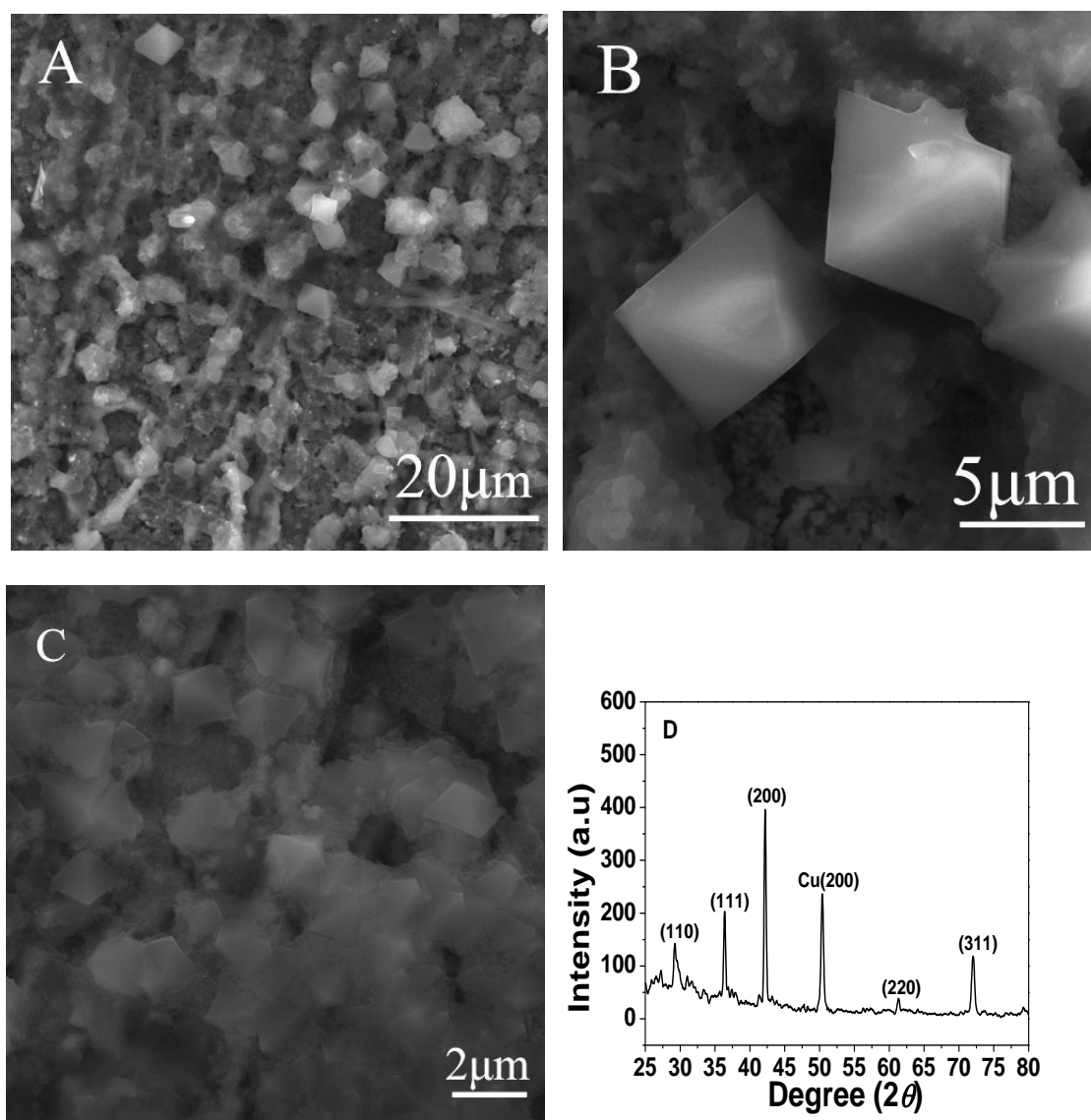
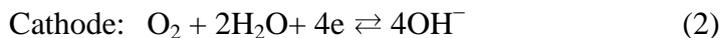


**Figure 1.** (A, B, C) SEM images with large scale (A scale bar 20  $\mu\text{m}$ ) and high magnification (B scale bar 5  $\mu\text{m}$  and C scale bar 2  $\mu\text{m}$ ). (D) XRD patterns of the  $\text{Cu}_2\text{O}/\text{Cu}$  electrode. The applied voltage and time to prepare  $\text{Cu}_2\text{O}/\text{Cu}$  electrode was 5 V and 5 s.

During the preparation process of the target electrode we found that the acid solution turned into alkaline, which illustrated that  $\text{OH}^-$  was produced in this process. The reaction solution in original colorless turned into blue which indicated that during the preparation of the electrode there were large

amounts of  $\text{Cu}^{2+}$  produced. Furthermore, the XRD characterization shows that the product is  $\text{Cu}_2\text{O}$ . According to these several factors we proposed the reaction mechanism might as [38–39]:



The electrochemical behaviors of the  $\text{Cu}_2\text{O}/\text{Cu}$  electrode were investigated by CVs at different scan rates in 0.1 M NaOH solution as shown in Fig. 2A. A wide oxidation peak at about 0.40–0.70 V was found, which was attributed to the oxidation of Cu (II) into Cu (III) [40]. The cathodic peak located at 0.60–0.70 V was ascribed to the reduction of the Cu(III) [40]. It was obvious that the peak current was enhanced and the reduction potential shifted negatively with the increased scan rate. The peak current are proportional to the scan rate during 0.02–0.20  $\text{V s}^{-1}$  (Fig. 2B), indicating that the electron transfer reaction involved with a surface–confined process.

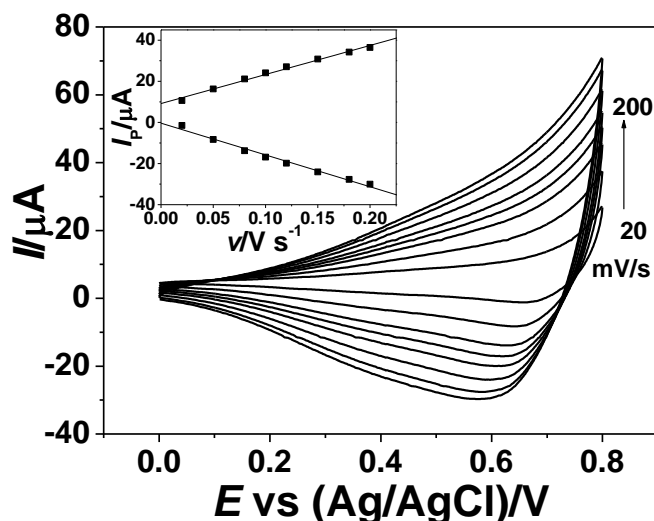
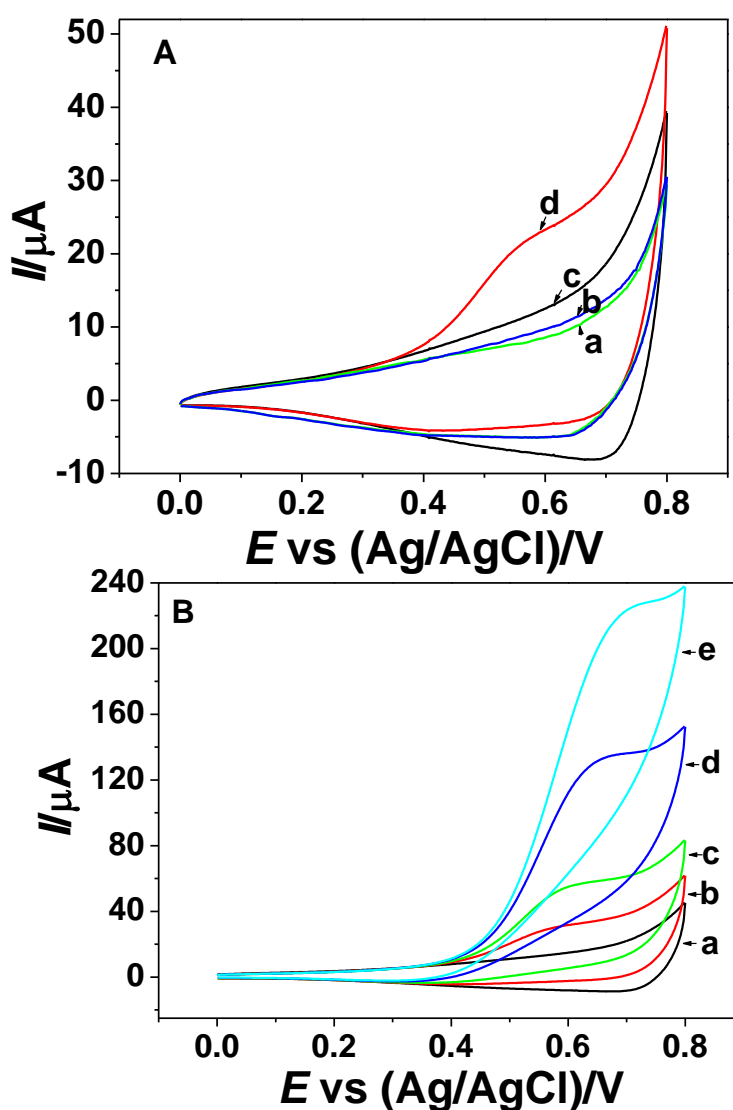


**Figure 2.** CVs of the  $\text{Cu}_2\text{O}/\text{Cu}$  electrode in 0.1 M NaOH at different scan rates (from bottom: 0.02, 0.05, 0.08, 0.10, 0.12, 0.15, 0.18 and 0.20  $\text{V s}^{-1}$ ). Inset: Plot of oxidation and reduction peak current (at 600 mV) versus the scan rate of 0.02–0.20  $\text{V s}^{-1}$ .

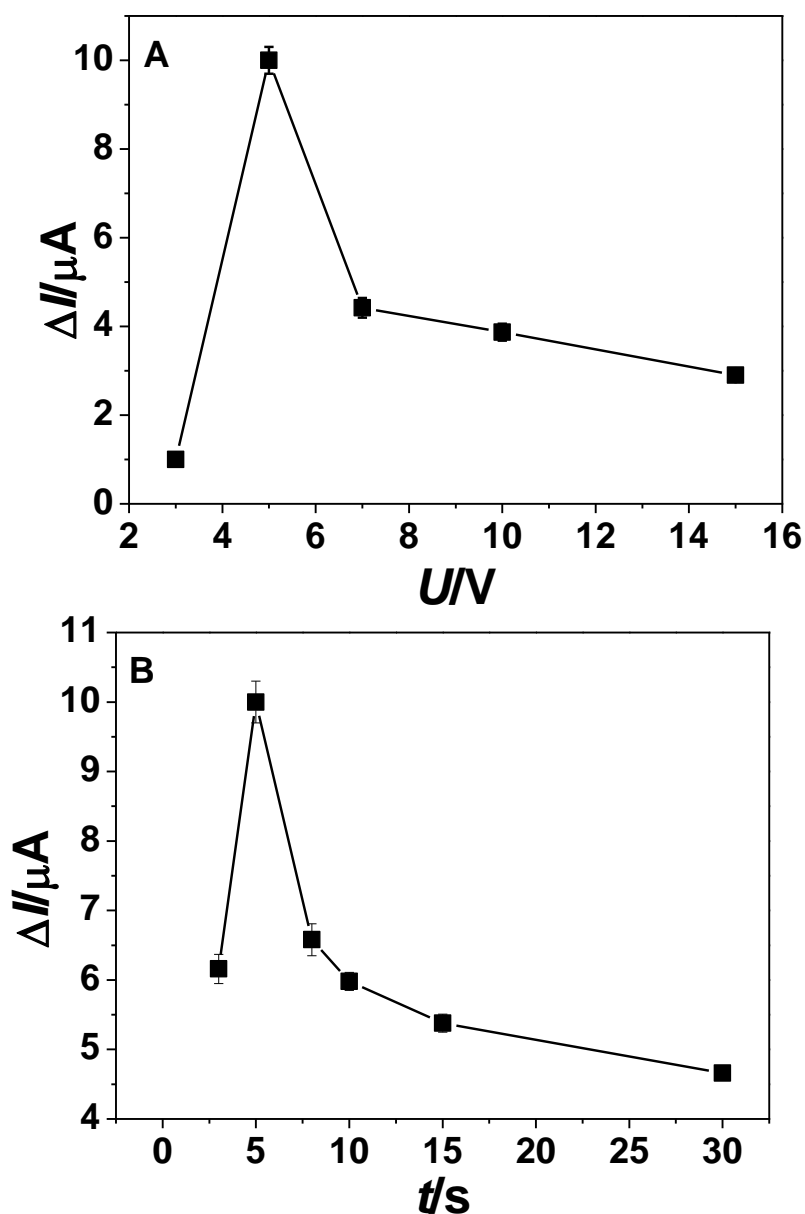
### 3.2 Electrocatalytic oxidation of glucose on the $\text{Cu}_2\text{O}/\text{Cu}$ electrode

The electrocatalytic activity of the bare Cu and  $\text{Cu}_2\text{O}/\text{Cu}$  electrode towards the oxidation of glucose in 0.1 M NaOH were shown in Fig. 3A. In the presence of 1.0 mM glucose, there was no

obvious catalytic oxidation current on the bare Cu electrode (curve b) as compared with that in the absence of glucose (curve a), while the  $\text{Cu}_2\text{O}/\text{Cu}$  electrode showed obvious catalytic oxidation current and a substantially negative shift in peak potential (curve d) in the presence of 1.0 mM glucose as compared with that in the absence of glucose (curve c). And the catalytic oxidation current was significantly higher than that of the bare Cu electrode. These results indicated that the produced  $\text{Cu}_2\text{O}$  microcrystal exhibited good electrocatalytic ability for the oxidation of glucose. The high electrocatalytic activity of the  $\text{Cu}_2\text{O}$  microcrystal in the catalytic oxidation of glucose was also confirmed by the obvious decrease in the anodic overpotential. The negative shift of the overpotential can be ascribed to a kinetic effect by an increase in the electroactive surface area and the electron transfer rate from the glucose to the  $\text{Cu}_2\text{O}/\text{Cu}$  electrode [41]. With the increasing of glucose concentration, the catalytic currents increased gradually on the  $\text{Cu}_2\text{O}/\text{Cu}$  electrode (Fig. 3B).



**Figure 3.** (A) CVs of Cu electrode (a and b) and  $\text{Cu}_2\text{O}/\text{Cu}$  electrode (c and d) in the absence (a and c) and presence (b and d) of 0.5 mM glucose in 0.10 M NaOH. (B) CVs of the  $\text{Cu}_2\text{O}/\text{Cu}$  electrode in 0.1 M NaOH in the presence of glucose: 0 (a), 1.0 (b), 2.0 (c), 4.0 (d) and 5.0 (e) mM. Scan rate:  $0.05 \text{ mVs}^{-1}$ . The applied voltage and time to prepare  $\text{Cu}_2\text{O}/\text{Cu}$  electrode was 5 V and 5 s.



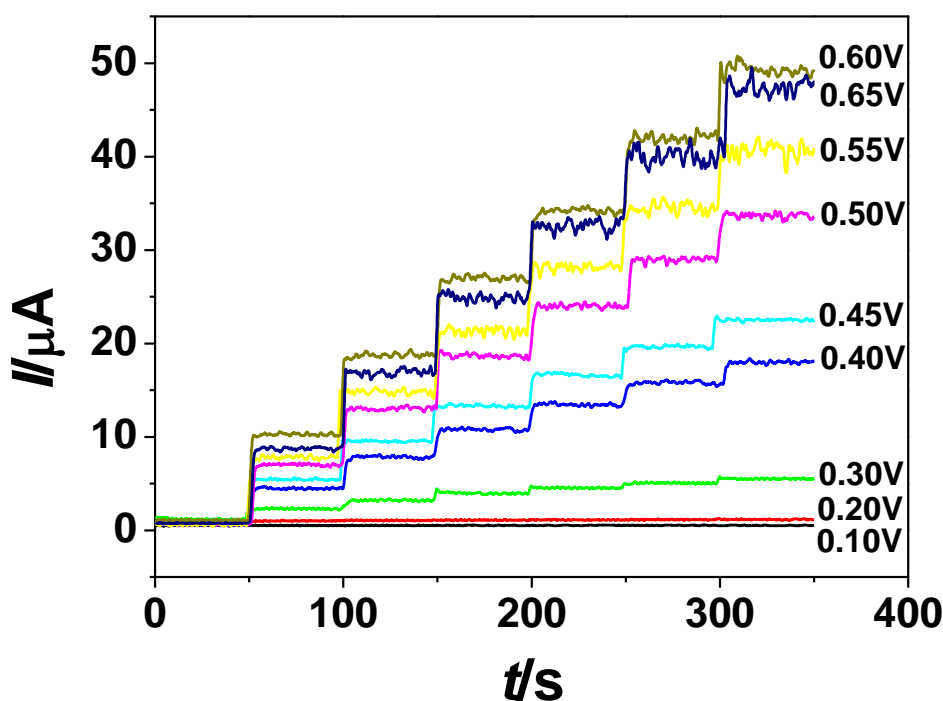
**Figure 4.** Plots of catalytic oxidation current ( $\Delta I = I_{\text{cat}} - I$ ) versus the applied voltage (the applied time is 5 s) (A) and time (the applied voltage is 5 V) (B) to prepare the  $\text{Cu}_2\text{O}/\text{Cu}$  electrode. The  $I_{\text{cat}}$  and  $I$  were the current value presence and in absence glucose, respectively.

Fig. 4A showed the effect of the applied voltage to prepare the  $\text{Cu}_2\text{O}/\text{Cu}$  electrode on the catalytic oxidation current. The catalytic oxidation current increased gradually with the increasing of the applied voltage from 3 V to 5 V. After the applied voltage exceeded 5 V, the catalytic oxidation current decreased gradually. This turning point might be ascribed to the fact that the  $\text{Cu}_2\text{O}$  microcrystal would become rather bigger with excessively high applied potential, which would decrease its electrochemical behaviors. The influence of  $\text{Cu}_2\text{O}/\text{Cu}$  electrode preparation time was also optimized here. As shown in Fig. 4B, the maximal value of the current response occurred at 5 s. This

phenomenon might be ascribed to the following two factors. On one hand, only a few  $\text{Cu}_2\text{O}$  microcrystals produced on the Cu electrode and the  $\text{Cu}_2\text{O}$  microcrystal was imperfect at a short time. On the other hand, the  $\text{Cu}_2\text{O}$  microcrystals would become rather bigger with the extension of time, which would result in the decrease of current response in reverse. Thus 5 s was chosen as the optimal preparation time here.

### 3.3 Chronoamperometric response and calibration curve

In order to study the effect of working potential on the electrocatalytic oxidation of glucose at the  $\text{Cu}_2\text{O}/\text{Cu}$  electrode, the amperometric responses to six successive injection of 0.5 mM glucose was recorded at different applied potentials varied from 0.10 to 0.65 V. As can be seen from Fig. 5, a small stepwise current response to the injection of glucose was observed after the applied potential was increased to 0.30 V, suggesting that the oxidation of glucose at the  $\text{Cu}_2\text{O}/\text{Cu}$  electrode started at around 0.30 V. The current response increased with the increase of working potential and reached the maximal value at 0.60 V. Thus 0.60 V was chosen as the working potential in the following experiments.



**Figure 5.** Electrocatalytic oxidation of 0.5 mM glucose on the  $\text{Cu}_2\text{O}/\text{Cu}$  electrode at different applied potentials (vs.  $\text{Ag}/\text{AgCl}$ ).

The catalytic rate constant ( $K_{\text{cat}}$ ) on the as-prepared  $\text{Cu}_2\text{O}/\text{Cu}$  electrode was measured with double steps chronoamperograms by setting the working electrode potentials to proper values [42,43]. Fig. 6A show double steps chronoamperograms for the  $\text{Cu}_2\text{O}/\text{Cu}$  electrode in the absence (curve a) and

presence (curve b: 5 mM, curve c: 10 mM, curve d: 15 mM) of glucose. The applied potential steps were 0.60 V and 0.30 V, respectively. Plot of net current with respect to the minus square roots of time was shown in Fig. 6B, presenting a linear dependency. It demonstrated that the electrocatalytic oxidation of glucose was a diffusion-controlled process. The diffusion coefficient ( $D$ ) of glucose could be estimated according to Cottrell equation [44]:

$$I = nFAD^{\frac{1}{2}}C\pi^{-\frac{1}{2}}t^{-\frac{1}{2}} \tag{6}$$

where  $n$  is the electron transfer number,  $F$  is the Faraday constant ( $F = 96487 \text{ C mol}^{-1}$ ),  $A$  is the effective surface area of electrode,  $C$  is the bulk concentration of glucose and other symbols have their usual meaning. Assumed the  $n$  value of 1 [40], the mean value of the diffusion coefficient of glucose was estimated to be  $5.66 \times 10^{-5} \text{ cm}^2 \text{ s}^{-1}$  by using the slope of the line in Fig. 6B.

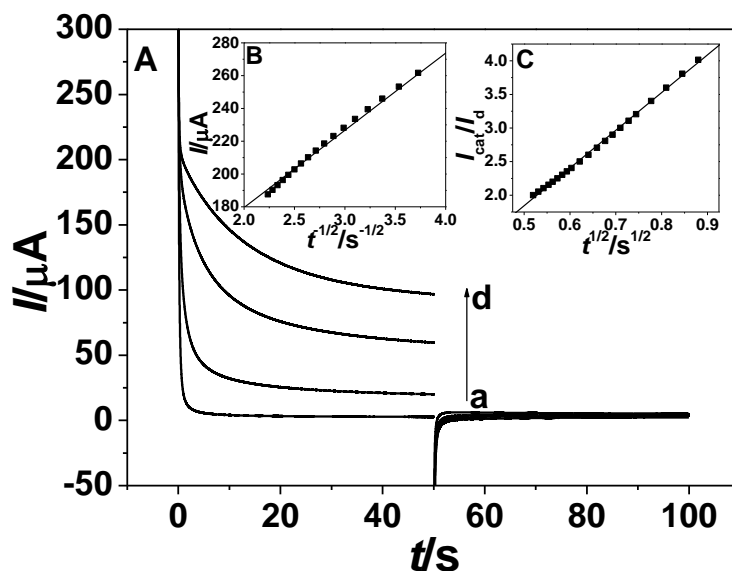


**Figure 6.** (A) Double steps chronoamperograms of the  $\text{Cu}_2\text{O}/\text{Cu}$  electrode in 0.1 M NaOH with different concentrations of glucose: 0 (a), 5 (b), 10 (c) and 15 (d) mM. Potential steps were 0.60V and 0.30V, respectively. (B) Dependency of transient current on  $t^{-1/2}$ . (C) Dependency of  $I_{\text{cat}}/I_{\text{d}}$  on  $t^{1/2}$  derived from the data of chronoamperograms of a and b in panel (A).

Chronoamperometry was also used for the evaluation of the catalytic rate constant with the help of the following equation [44]:

$$\frac{I_{\text{cat}}}{I_{\text{d}}} = \lambda^{\frac{1}{2}} \left[ \frac{1}{\pi^2} \text{erf}(\lambda^{\frac{1}{2}}) + \frac{\exp(-\lambda)}{\lambda^{\frac{1}{2}}} \right] \tag{7}$$

where  $I_{\text{cat}}$  and  $I_{\text{d}}$  are the currents in the presence and absence of glucose,  $\lambda = K_{\text{cat}}Ct$  is the argument of the error function,  $K_{\text{cat}}$  is the catalytic rate constant and  $t$  is the consumed time. In the case where  $\lambda > 1.5$ ,  $\text{erf}(\lambda^{1/2})$  is almost equal to unity, the above equation can be reduced to:

$$\frac{I_{\text{cat}}}{I_{\text{d}}} = \lambda^2 \pi^2 = \pi^2 (K_{\text{cat}}Ct)^2 \quad (8)$$

From the slope of the  $I_{\text{cat}}/I_{\text{d}}$  versus  $t^{1/2}$  plot, as shown in Fig. 6C, the mean value of  $K_{\text{cat}}$  for glucose was calculated as  $4.02 \times 10^4 \text{ cm}^3 \text{ mol}^{-1} \text{ s}^{-1}$ . All of the kinetic parameters obtained in this work are summarized in Table 1.

**Table 1.** Comparison of the performance of the  $\text{Cu}_2\text{O}/\text{Cu}$  electrode with other glucose sensors based on different Cu materials.

Electrode	Detection potential V	$D$ $\text{cm}^2 \text{ s}^{-1}$	$K_{\text{cat}}$ $\text{cm}^3 \text{ mol}^{-1} \text{ s}^{-1}$	Detection limit $\text{mmol L}^{-1}$	Linear range mM	Slope $\mu\text{A mmol L}^{-1} \text{cm}^{-2}$	References
$\text{Cu}_2\text{O}/\text{Cu}$	0.6 (vs. Ag/AgCl)	$5.66 \times 10^{-5}$	$4.02 \times 10^4$	0.037	0.05–6.75	$62.29 \mu\text{A mmol L}^{-1}$	This work
Nafion/CuO/GC	0.6 (vs. Ag/AgCl)	–	–	0.001	0–2.55	404.53	[45]
CuO nanorod	0.6 (vs. SCE)	–	–	0.0012	Up to 1.0	450	[46]
CuO/TiO <sub>2</sub>	0.5 (vs. SCE)	–	–	0.001	Up to 2.0	79.79	[35]
Cu nanocluster/MWCNTs/GC electrode	0.65 (vs. Ag/AgCl)	$6.73 \times 10^{-6}$	–	0.00021	Up to 3.5	$17.76 \mu\text{A mmol L}^{-1}$	[16]
CuO–MWCNTs array electrode	0.55 (vs. SCE)	–	–	0.0008	Up to 3.0	2190	[15]
CuO nanorods–graphite electrode	0.60 (vs. Ag/AgCl)	–	–	0.004	Up to 8.0	371.4	[47]

Amperometric measurements were carried out at 0.60 V at the  $\text{Cu}_2\text{O}/\text{Cu}$  electrode by successive injection of glucose into a stirring 0.1 M NaOH (Fig. 7A). The oxidation current reached a maximum steady–state value and achieved 95% of the steady–state current in 5 s. It was noticeable that the noise increased with the increasing of glucose concentration. It was because that more and more intermediate species might adsorb onto the  $\text{Cu}_2\text{O}/\text{Cu}$  electrode as the glucose concentration increased and the reaction time prolonged. Fig. 7B showed the calibration curve of the sensor. The oxidation current was proportional to the concentration of glucose in the range of 0.05–6.75 mM ( $r=0.9985$ ) with a slope of  $62.29 \mu\text{A mM}^{-1}$ . The detection limit was estimated to be  $37 \mu\text{M}$  based on the criterion of a signal–to–noise ratio of 3.

Recently, many non–enzymatic glucose sensors based on copper or its oxide. A comparison of the performance of our glucose sensor with those reported in literatures was listed in Table 1. All of these sensors have their advantages and limitations. Generally, the detection limit was fairly low, the linear range was not wide some were even very narrow. Taking Cu nanocluster/MWCNTs/GC electrode [35] as an example, the detection limit was pretty low ( $0.21 \mu\text{M}$ ). However, the linear range was narrow (up to 3.5 mM). Besides, the diffusion coefficient was smaller than our as–prepared

Cu<sub>2</sub>O/Cu electrode. Although the detection limit of our sensor is not lowest, it's low enough for the routing inspection, and the linear range of ours is wider than others except the CuO nanorods–graphite electrode [49].

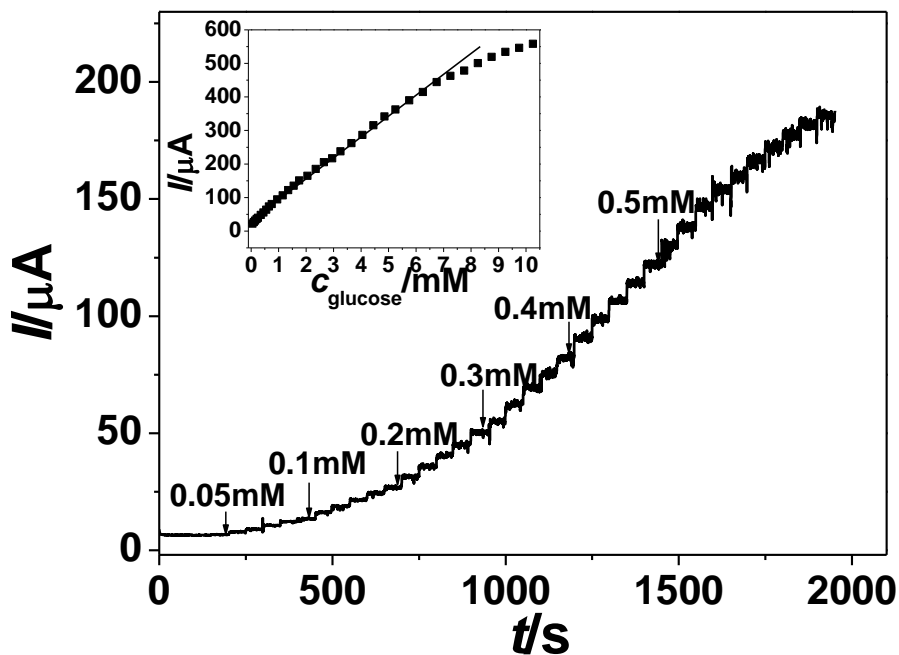


**Figure 7.** (A) Typical amperometric response of the Cu<sub>2</sub>O/Cu electrode to successive injection of glucose into the stirred 0.1 M NaOH. (B) The calibration curve. Applied potential: 0.60 V.

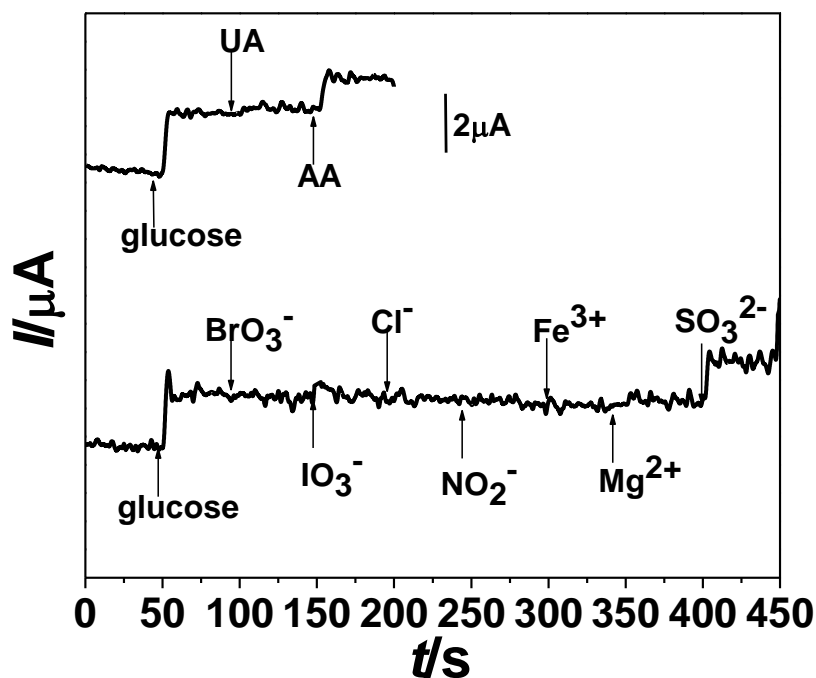


**Figure 8.** The interference effect of some electro-active substance on glucose detection. Applied potential: 0.60 V.

Interference is inevitable in the determination of some analyses. Some interference was also investigated here as shown in Fig. 8. Chemicals such as  $\text{BrO}_3^-$ ,  $\text{IO}_3^-$ , uric acid,  $\text{NO}_2^-$ ,  $\text{Mg}^{2+}$ ,  $\text{Cl}^-$  and  $\text{Fe}^{3+}$  in a 10-fold concentration did not show obvious interference to glucose detection, while  $\text{SO}_3^{2-}$ , and ascorbic acid in a 2-fold concentration interfered significantly. These results implied the good selectivity of the sensor.

#### 3.4 Stability, repeatability and reproducibility of $\text{Cu}_2\text{O}/\text{Cu}$ electrode

The stability, repeatability and reproducibility of the resulted sensor were also investigated in this work. After the sensor was stored at room temperature for 7 days, the current response to 0.1 mM glucose decreased 1.85% of the original current. The repeatability of successive amperometric measurements for five different 0.1 mM glucose carried out with the same biosensor was checked. A relative standard deviation value (RSD) of 2.47% was calculated for the steady current. The reproducibility of the response to 0.1 mM glucose obtained with five different biosensors was also evaluated with a RSD of 2.2%.

## 4. CONCLUSIONS

In this work, a facile strategy to prepare  $\text{Cu}_2\text{O}/\text{Cu}$  electrode as a sensitive nonenzymatic glucose sensor was developed by an electrochemical method, which avoided the tedious of synthetic materials and the construction of electrode as the traditional sensor and realized the synthesis of materials and firmly immobilization in one step. The SEM images show that ultrafine octahedron  $\text{Cu}_2\text{O}$  microcrystal was prepared and densely assembled on Cu electrode. The electrode exhibits large surface area and shows a high electrocatalytic behavior toward the oxidation of glucose. The sensor has the advantages of simple and convenient preparation, low production cost, good electrocatalytic activity, high stability and low detection limit. It is possible to be a potential candidate for routine glucose analysis.

## ACKNOWLEDGMENTS

This work was financially supported by National Natural Science Foundation of China (20905032, 21065005, 21165010), Young Scientist Foundation of Jiangxi Province (20112BCB23006; 20122BCB23013), Foundation of Jiangxi Educational Committee (GJJ10389), State Education Ministry and the Open Project Program of Key Laboratory of Functional Small organic molecule (No. KLFS-KF-201214; KLFS-KF-01218).

## References

1. A. Heller, and B. Feldman, *Chem. Rev.*, 108(2008) 2482.
2. K. E. Toghill and R. G. Compton, *Int. J. Electrochem. Sci.*, 5(2010) 1246.
3. J. Wang, *Chem. Rev.*, 108(2008) 814.

4. L. Bahshi, R. Freeman, R. Gill and I. Willner, *Small*, 5(2009)676.
5. M. Zheng, Y. Cui, X.Y. Li, S.Q. Liu and Z. Y. Tang, *J. Electroanal. Chem.*, 656(2010) 167.
6. W. Wu, S. Chen, Y. Hu and S. Zhou, *J. Diabetes Sci. Technol.*, 33(2012) 892.
7. H. Noh, K. Lee, P. Chandra, M. Won and Y. Shim, *Electrochim. Acta*, 61(2012)36..
8. W. T. Wu, J. Shen, Y. X. Li, H. B. Zhu, P. Banerjee and S. Q. Zhou, *Biomaterials*, 33(2012) 7115.
9. O. Yehezkeli, R. Tel-Vered, S. Reichlin and I. Willner, *ACS Nano*, 5(2011)2385.
10. X. Li, Q. Y. Zhu, S. F. Tong, W. Wang, W. B. Song, *Sensor. Actuat. B-Chem.*, 136(2009) 444.
11. Y. M. Yan, R. Tel-Vered, O. Yehezkeli, Z. Cheglakov and I. Willner, *Adv. Mater.*, 20(2008) 2365.
12. M. Gu, J. Wang, Y. Tu and J. Di, *Sensor. Actuat. B-Chem.*, 148(2010) 486.
13. X. Y. Li, Y. L. Zhou, Z. Z. Zheng, X. L. Yue, Z. F. Dai, S. Q. Liu and Z. Y. Tang, *Langmuir*, 25(2009) 6580.
14. Y. M. Yan, I. Baravik, O. Yehezkeli and I. Willner, *J. Phys. Chem. C*, 112(2008) 17883.
15. J. Yang, L. C. Jiang, W. D. Zhang and S. Gunasekaran, *Talanta*, 58(2010) 25.
16. X. H. Kang, Z. B. Mai, X. Y. Zou, P. X. Cai and J. Y. Mo, *Anal. Biochem.*, 363(2007) 143.
17. J. Wang and W. Zhang, *Electrochim. Acta*, 56(2011)7510.
18. W. Wang, Z. Li, W. Zheng, J. Yang, H. Zhang and C. Wang, *Electrochem. Commun.*, 11(2009) 1811.
19. T. G. Satheesh Babu and T. Ramachandran, *Electrochim. Acta*, 55(2010)1612.
20. J. Luo, S. Jiang, H. Zhang, J. Jiang and X. Liu, *Anal. Chim. Acta*, 709(2012) 47.
21. L. Luo, L. Zhu and Z. Wang, *Bioelectrochemistry*, 88(2012) 156.
22. J. Chen, W. Zhang and J. Ye, *Electrochem. Commun.*, 10(2008)1268.
23. Y. Zhang, Y. Wang, J. Jia and J. Wang, *Sensor. Actuat. B-Chem.*, 171–172(2012) 580.
24. R. Ahmad, N. Tripathy, J. H. Kim, Y.-B. Hahn, *Sensor. Actuat. B-Chem.*, 174(2012) 195.
25. X. Zhang, G. Wang, W. Zhang, N. Hu, H. Wu and B. Fang, *J. Phys. Chem. C*, 112 (2008) 8856.
26. A.J. Wang, J.J. Feng, Z.H. Li, Q.C. Liao, Z.Z. Wang and J.R. Chen, *CrysEngComm*, 14 (2012) 1289.
27. T. Soejima, H. Yagyu, N. Kimizuka and S. Ito, *RSC Adv.*, 1 (2011) 187.
28. H. Pang, Q. Lu, J. Wang, Y. Li and F. Gao, *Chem. Commun.*, 46 (2010) 2010.
29. X. Zhang, A. Gu, G. Wang, Y. Wei, W. Wang, H. Wu and B. Fang, *CrysEngComm*, 12 (2010) 1120.
30. X. Zhang, G. Wang, A. Gu, Y. Wei and B. Fang, *Chem. Commun.*, 44 (2008) 5945.
31. J. Liu and D. Xue, *J. Mater. Chem.*, 21 (2011) 223.
32. Z. Zhuang, X. Su, H. Yuan, Q. Sun, D. Xiao and M. M. F. Choi, *Analyst*, 133 (2008) 126.
33. S. Liu, J. Tian, L. Wang, X. Qin, Y. Zhang, Y. Luo, A. M. Asiri, A. O. Al-Youbi and X. Sun, *Catal. Sci. Technol.*, 2 (2012) 813.
34. S. Prakash and V. Shahi, *Anal. Methods*, 3 (2011) 1331.
35. S.L. Luo, F. Su, C.B Liu, J.X. Li, R.H. Liu, Y. Xiao, Y. Li, X.N Liu and Q.Y Cai, *Talanta*, 86 (2011) 157.
36. X. Zhou, H. Nie, Z. Yao, Y. Dong, Z. Yang and S. Huang, *Sensor. Actuat. B-Chem.*, 168(2012) 1.
37. X. Ye, Y. Gu and C. Wang, *Sensor. Actuat. B-Chem.*, 173(2012) 530.
38. L. Wang, G. Liu and D. Xue, *Electrochim. Acta*, 56(2011)6277.
39. H. S. Shin, J. Y. Song, J. Yu, *Mater. Lett.*, 63(2009)397.
40. H.X. Wu, W.M. Cao, Y. Li, G. Liu, Y. Wen, H.F. Yang and S.P. Yang, *Electrochim. Acta*, 55 (2010) 3734.
41. L.C. Jiang and W.D. Zhang, *Biosens. Bioelectron.*, 25 (2010) 1402.
42. Y. Song, Z. He, H. Hou, X. Wang and L. Wang, *Electrochim. Acta*, 71(2012)58.
43. Y. Song, Z. He, H. Zhu, H. Hou and L. Wang, *Electrochim. Acta*, 58(2011) 757.
44. A. J. Bard and L. R. Faulkner, John Wiley and Sons (2011) *Electrochemical Methods*, Inc New York.
45. E. Reitz, W.Z. Jia, M. Gentile, Y. Wang and Y. Lei, *Electroanal.*, 20(2008) 2482.

46. C. Batchelor–McAuley, Y. Du, G. G. Wildgoose and R. G. Compton, *Sensor. Actuat. B–Chem.*, 135(2008) 230.
47. X. Wang, C. Hu, H. Liu, G. Du, X. He and Y. Xi, *Sensor. Actuat. B–Chem.*, 144(2010) 220.